Journal of Applied Polymer Science

Compatibility, steady and dynamic rheological behaviors of polylactide/poly(ethylene glycol) blends

Feng-Jiao Li,[1,2] Ling-Cao Tan,[1] Shui-Dong Zhang,[1,2] Bo Zhu[1]

[1]School of Mechanical and Automotive Engineering, South China University of Technology, Guangzhou 510640, People's Republic of China

[2]Key Laboratory of Polymer Processing Engineering of the Ministry of Education, South China University of Technology, Guangzhou 510640, People's Republic of China

Correspondence to: S.-D. Zhang (E-mail: starch@scut.edu.cn)

ABSTRACT: Understanding the rheological behavior of plasticized polylactide (PLA) contributed to the optimization of processing conditions and revealed the microstructure–property relationships. In this study, the morphological, thermal, steady and dynamic rheological properties of the PLA/poly(ethylene glycol) (PEG) blends were investigated by scanning electron microscope, differential scanning calorimeter, and capillary and dynamic rheometers, respectively. The results illuminated that the melt shear flow basically fitted the power law, whereas the temperature dependence of the apparent shear viscosity (η_a) or complex viscosity (η^*) followed the Arrhenius equation. Both the neat PLA and PLA/PEG blends exhibited shear-thinning behavior. Because the incorporation of PEG reduced the intermolecular forces and improved the mobility of the PLA chains, the η_a, η^*, and storage and loss moduli of the PLA/PEG blends decreased. The PEG content (W_{PEG}) ranged from 0 to 10 wt%, both η_a and η^* decreased significantly. However, the decrements of η_a and η^* became unremarkable when W_{PEG} exceeded 10 wt %. The reason was attributed to the occurrence of phase separation, which resulted in the decrease in the plasticization and lubrication efficiencies. This study demonstrated that the addition of the right amount of PEG obviously improved the flow properties of PLA. © 2015 Wiley Periodicals, Inc. J. Appl. Polym. Sci. **2016**, *133*, 42919.

KEYWORDS: compatibility; PLA/PEG blends; plasticization; rheological properties

Received 3 July 2015; accepted 5 September 2015

DOI: 10.1002/app.42919

INTRODUCTION

In recent years, with the aggravation of energy crisis and environmental pollution, polylactide (PLA) has increasingly attracted attention as one of the most promising renewable, biodegradable, and compostable thermoplastic polyesters.[1,2] Because of its excellent biodegradability, biocompatibility, bioabsorbability, transparency, high strength and modulus, energy savings, low toxicity, and easy processability, PLA shows vast potential for applications in many fields, such as in biomedical devices, packaging, and automotive industries.[1–5] Furthermore, it also has the potential to replace some nondegradable petroleum-based polymers in various disposable or short-term applications, such as disposable tableware (e.g., bottles, cups, plates, fast food boxes), food wrapping, bags, and agricultural mulch films.[6–8] However, unfortunately, the inherent brittleness and poor toughness of PLA have restricted its large-scale biomedical and packaging applications. The reason is that biomedical applications such as bone screws and fracture fixation plates are needed to withstand plastic deformation at higher stress levels.[1,9] Additionally, a high flexibility at room temperature is an important requirement for packaging materials such as films. To improve the flexibility and extend the application range of PLA, the blending of PLA with rubbers,[3,10] flexible polymers [e.g., poly(ε-caprolactone),[11] polyurethane,[12,13] poly(butylene succinate),[14] poly(butylene adipate-*co*-terephthalate)[15]], elastomers (e.g., bioelastomer,[16] polyamide elastomer[17]), or various plasticizers [e.g., glycerol,[18] oligomeric lactic acid,[18] poly(ethylene glycol) (PEG),[19] poly(propylene glycol),[20] citrate esters,[21] and glucose monoesters[22]] is a simple, feasible, and effective method.

As an efficient plasticizer for PLA, PEG is a linear or branched hydroxyl-terminated polyether, which is usually prepared by anionic ring-opening polymerization of ethylene oxide.[23] Its merits include excellent lubricity, plasticity, dispersibility, high mobility and hydrophilicity, good biocompatibility, nontoxicity, and so on. Moreover, PEG melts exhibit Newtonian fluid behaviors above their melting points.[24] Because of its aforementioned advantages, PEG has been broadly applied in various fields, such as cosmetic, pharmaceutical, biomedicine, food processing.[23,24]

It is generally considered that PEG has good compatibility with PLA. The reason is that the terminal hydroxyl groups of PEG molecules can react with the carboxyl groups of PLA molecules. The incorporation of right amount of PEG can not only greatly enhance the flexibility, ductility, impact strength, and hydrophilicity of PLA, but also accelerate the biodegradation of PLA. Meanwhile, the introduction of PEG can still retain the biocompatibility, biodegradability, and food contact applications of PLA owing to the biocompatibility, biodegradability, and nontoxicity of PEG. Hence, on the basis of the above analysis, PEG is an excellent plasticizer which can remarkably improve the mobility of PLA chains and the elongation at break of PLA.[19]

Recently, many studies have focused on the miscibility, mechanical, thermal, and rheological properties of plasticized PLA-based blends. Jacobsen and Fritz[22] surveyed the influence of the content and type of three different plasticizers {i.e., PEG (weight-average molecular weight (M_w) = 1.5 × 10^3], glucose monoesters, and partial fatty acid esters} on the mechanical properties of PLA. For these three PLA/plasticizer blend systems, the elastic modulus and tensile strength decreased, whereas the elongation at break increased with increasing plasticizer content. When the contents of these three plasticizers were 10 wt %, the introduction of PEG led to the largest declines in the glass-transition temperature (T_g; it declined nearly 30 K), elastic modulus, and tensile strength, while the biggest increases in the elongation at break (up to 180%) and impact strength when compared with the two other plasticizers. These results indicated that PEG was a highly effective plasticizer for PLA. Sheth *et al.*[24] investigated the effect of the PEG (M_w = 2.0 × 10^4) content on the miscibility and mechanical properties of the PLA/PEG blends. They noticed that the miscibility of PEG with PLA varied between complete miscibility and partial miscibility, depending on the PEG content (W_{PEG}). When W_{PEG} was less than 50 wt %, the tensile strength and modulus of the blends decreased, whereas the strain at break increased with increasing W_{PEG}. Nevertheless, when W_{PEG} exceeded 50 wt %, the blend crystallinity increased; this led to an increase in the tensile modulus and a significant decrease in the strain at break of the PLA/PEG blends. In addition, they also found that both PEG and PLA in the blends crystallized and the introduction of PEG improved the crystallization of PLA. Sungsanit *et al.*[19] plasticized linear PLA (L-PLA) with PEG (M_w = 1000). They found that the PEG phase separated from the L-PLA/PEG blends when W_{PEG} was higher than 10 wt %, this was exactly the reason that the blends became brittle at relatively high W_{PEG} values. The rheological results indicated that both the neat L-PLA and L-PLA/PEG blends showed a slight shear-thinning behavior in the oscillation frequency (ω) range 0.1–100 rad/s. In addition, the viscosities, storage modulus (G') and loss modulus (G'') of the blends decreased with increasing W_{PEG} for all frequencies. However, in the low-ω region, the effect of ω on G' was inconspicuous with increasing W_{PEG}.

It is well-known that the rheological behaviors of polymer melts play a vital role in processing and determining the morphology and mechanical properties of final products. Therefore, fully understanding the rheological properties of plasticized PLA blends is crucial to optimizing the processing conditions and improving the performances of the PLA-based products. Over the last 3 decades, rheological characterization has been applied to explore the relationship between the viscoelastic properties and phase separation of polymer blends. According to rheological measurements, particularly dynamic tests, many fingerprints can be determined to qualitatively or quantitatively deduce the critical point of phase transition in polymer blends.[25] Utracki[26] pointed out that rheological behavior measurement under small-amplitude oscillatory shear was an optimal approach for characterizing the phase behavior of polymer blends. Zheng *et al.*[27] investigated the correlation between the dynamic rheological behavior and phase separation of poly(methyl methacrylate)/poly(styrene-*co*-acrylonitrile) blends. Li *et al.*[28] studied the effect of the content of functionalized multiwalled carbon nanotubes (FMWCNTs) on the dynamic rheological properties of poly(L-lactide)/PEG/FMWCNTs nanocomposites. However, surprisingly, so far there have been very few reports on the effect of W_{PEG} on the steady and dynamic rheological behaviors of PLA/PEG blends, especially on the use of a dynamic rheological method to analyze the phase separation of PLA/PEG blends. To better grasp the rheological behaviors and mechanisms of PLA/PEG blend melts, and to provide useful guidance for optimizing process conditions and enhancing the performances of PLA/PEG blending products, the main focus of this study was the adoption of a dynamic rheological method to study the phase separation of PLA/PEG blends. We hoped to reveal the relationship between the structure and properties through rheological measurements and to optimize the processing conditions by systematically evaluating the effects of W_{PEG}, shear rate, ω, and test temperature on the rheological properties of the PLA/PEG blends.

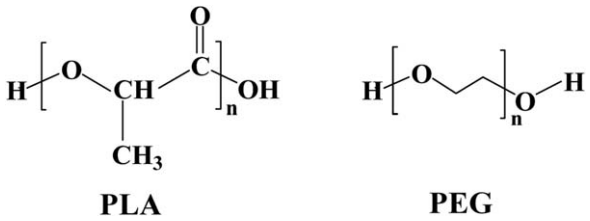

Figure 1. Structural formulas of PLA and PEG.

EXPERIMENTAL

Materials

PLA with the trademark of Ingeo 4032D was supplied by NatureWorks LLC. It contained about 2 wt % D-isomer, and its M_w, density, T_g, and melting temperature (T_m) were 190,000, 1.24 g/cm^3, 59.2°C, and 170°C, respectively.

PEG (guaranteed reagent grade) was used as a plasticizer for PLA and was purchased from Sinopharm Chemical Reagent Co., Ltd. (Shanghai, China). Its average molecular weight was 6000. The structural formulas of PLA and PEG are shown in Figure 1.

Sample Preparation

To minimize the hydrolytic degradation during melt mixing, PLA and PEG were first vacuum-dried at 80°C for 4 h and 45°C for 8 h, respectively. Then, the PEG was premixed with PLA at 5, 10, 15, and 20 wt %, and the PLA/PEG mixtures were

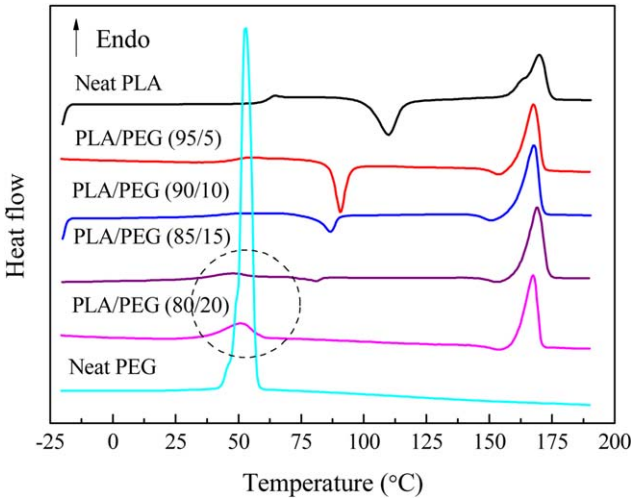

Figure 2. DSC thermograms of the second heating of the neat PLA and PLA/PEG blends at a heating rate of 10°C/min. [Color figure can be viewed in the online issue, which is available at wileyonlinelibrary.com.]

subsequently melt-extruded with an SHJ-26 corotating twin screw extruder at a screw rotation speed of 230 rpm in the temperature range 160–180°C. The diameter (D) and length (L)-to-D ratio of the screw were 26 mm and 40:1, respectively. For better comparison, the neat PLA was also melt-extruded under the same conditions. Finally, the extrudates of the neat PLA and PLA/PEG blends were chopped into particles and dried again *in vacuo* at 45°C for 24 h before differential scanning calorimetry (DSC) analysis, steady rheological testing, and compression molding.

The disklike samples used for dynamic rheological tests were compression-molded by means of a daylight press operating at 180°C for 5 min under a pressure of 15 MPa. The thickness and D of the prepared disks were 1 and 25 mm, respectively. These test disks were dried at 45°C for 5 h before the dynamic rheological tests.

DSC

The compatibility of PLA/PEG blends was revealed with a differential scanning calorimeter (NETZSCH DSC 204F1 Phoenix, Germany) under an N_2 atmosphere. To erase the influence of any previous thermal history, each sample (ca. 5 mg) was first heated from 30 to 190°C at a heating rate of 10°C/min and maintained at 190°C for 5 min. Subsequently, all of the samples were cooled to −20°C at a cooling rate of 10°C/min and held at −20°C for 5 min. Finally, all of the samples were heated again from −20 to 190°C at a heating rate of 10°C/min. During the second heating scan, the T_g, cold crystallization temperature (T_{cc}), and T_m of the sample were obtained.

Scanning Electron Microscopy (SEM)

The dispersion of PEG in the PLA matrix and the compatibility of PLA and PEG were further explored with an S-3700N scanning electron microscope (Hitachi, Japan), operating at an acceleration voltage of 10 kV. Before SEM observations, all of samples from capillary extrusion at 180°C and a shear rate of 800 s^{-1} were cryogenically fractured in liquid nitrogen, and the fractured surfaces were coated with a thin layer of gold.

Steady-State Rheological Measurement

The steady shear rheological properties of the neat PLA and PLA/PEG blend melts were measured with a Rheologic 5000 capillary rheometer (CEAST Co., Italy). The apparent shear rate ($\dot{\gamma}_a$) and test temperature ranged from 25 to 4 × 10^3 s^{-1} and from 175 to 195°C, respectively. The capillary lengths (L) were 10, 20, and 40 mm, respectively, and the die D was 1 mm. Therefore, the corresponding L/D ratios were 10:1, 20:1, and 40:1, respectively. The entrance angles of these dies were 180°. The correlation between the ($\dot{\gamma}_a$) and volume flow rate (q_V) was expressed by eq. (1):

$$\dot{\gamma}_a = \frac{32 q_V}{\pi D^3} \quad (1)$$

The entrance pressure drop (ΔP_{en}) was determined by the Bagley correction method. The relationship between the wall shear stress (τ_R) and total pressure drop (ΔP) was given by eq. (2):

$$\tau_R = \frac{\Delta P - \Delta P_{en}}{4(L/D)} \quad (2)$$

Dynamic Rheological Measurement

The dynamic rheological properties of the neat PLA and PLA/PEG blends were tested by a Gemini 200 rheometer system (Bohlin Co., United Kingdom) in oscillation mode equipped with a 25 mm diameter parallel plate fixture. The tests were carried out at temperatures ranging from 175 to 195°C and frequency sweeps from 0.0628 to 628 rad/s at a constant strain amplitude of 1% to assure that the measurements were performed within the linear viscoelastic region.

RESULTS AND DISCUSSION

DSC Analysis of the Compatibility of PLA/PEG Blends

The compatibility between PEG and PLA was investigated by DSC analysis. Figure 2 shows the DSC thermograms of the second heating of the neat PLA and PEG and PLA/PEG blends, and the corresponding thermal characteristic data are summarized in Table I. Moreover, Cuénoud *et al.*[29] reported that T_g of PEG 6000 was −42°C. The combination of Table I with Figure 2, it can be seen that the PLA/PEG blends had only one T_g, which decreased from 59.2°C for neat PLA to 43.7°C for the PLA/PEG blend with 5 wt % PEG. Nevertheless, for the blends containing a higher W_{PEG}, T_g was nearly indistinguishable. Similarly, T_{cc} of the PLA/PEG blends decreased remarkably from 110.0 to 86.7°C when W_{PEG} ranged from 0 to 10 wt %, whereas T_{cc} slightly decreased or was no longer detected as W_{PEG} increased further. The single T_g and the significant reductions in T_g and T_{cc} of the PLA/PEG blends

Table I. DSC Data for the Neat PLA and PLA/PEG Blends

	Second heating		
W_{PEG} (wt %)	T_g (°C)	T_{cc} (°C)	T_m (°C)
0	59.2	110.0	170.0
5	43.7	90.7	167.6
10	—	86.7	167.7
15	—	84.4	168.4
20	—	—	167.4

T_{cc} and T_m were peak temperatures, whereas T_g was the onset temperature.

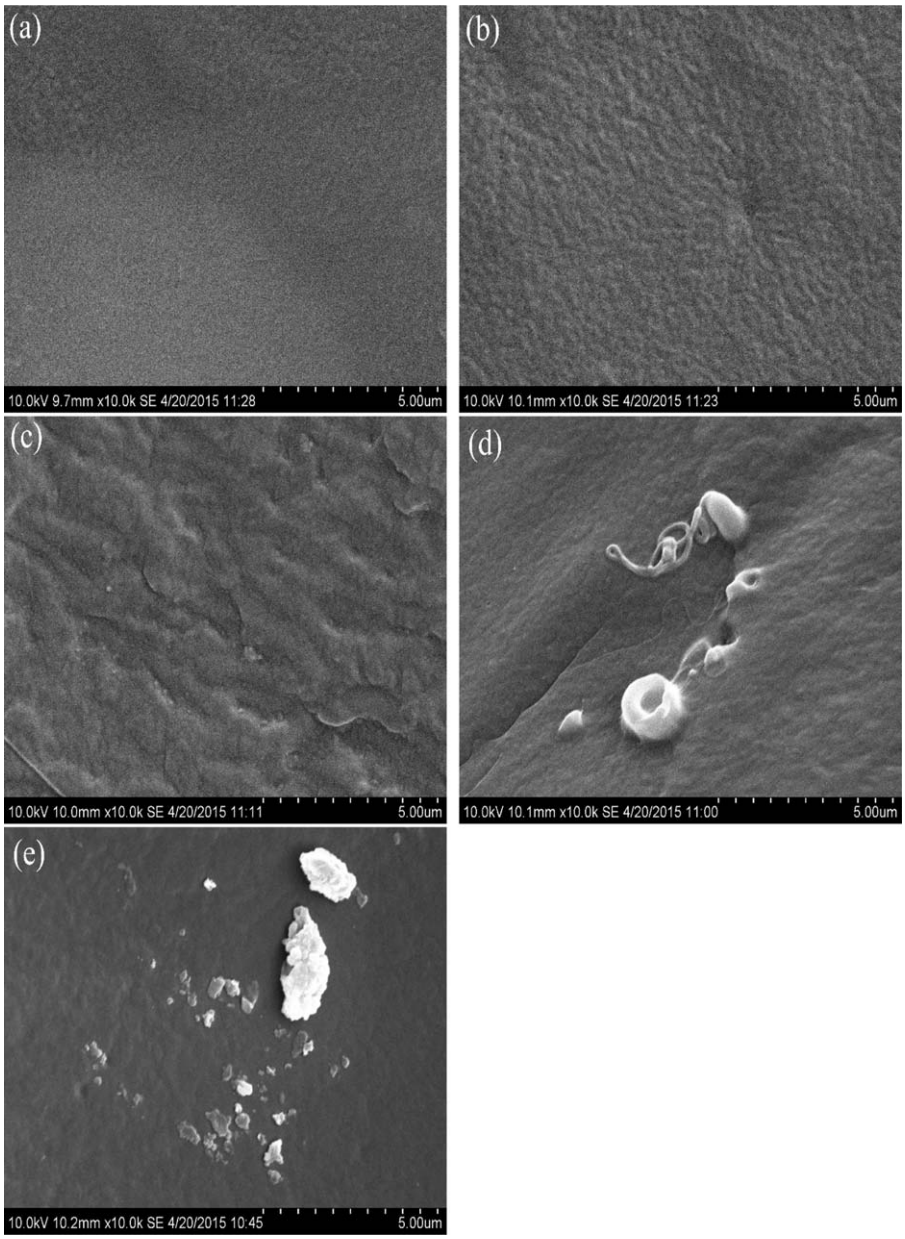

Figure 3. SEM micrographs of the PLA/PEG blends: (a) 100/0, (b) 95/5, (c) 90/10, (d) 85/15, and (e) 80/20.

demonstrated that PEG was miscible with PLA when W_{PEG} was less than 10 wt %. However, the small melting peaks of PEG were observed in the PLA/PEG blends when the W_{PEG}s were 15 and 20 wt %, respectively (see the circle part of Figure 2). Similar results were also observed in the thermal analysis of L-PLA/PEG 1000 blends by Sungsanit *et al.*[19] In a comparison with the melting peak of neat PEG, we speculated that the PEG phase might separate from the PLA/PEG blends, as was further confirmed by SEM.

Dispersion Morphology of PEG in the PLA/PEG Blends

In this study, SEM was applied to reveal the dispersion of PEG in the PLA matrix and the compatibility of PEG and PLA. As is well known, the dispersion degree of polymer/polymer binary blends is determined by the compatibility between the two compositions. Generally, the better the miscibility of two polymers is, the smaller the size of the disperse phase is and the more homogeneous the distribution of the dispersed phase in prepared blends is.[30] Figure 3 presents the SEM micrographs of the cryofractured surfaces of the neat PLA and PLA/PEG blends. We observed in Figure 3(b,c) that the PEG granules were homogeneously and finely dispersed in the PLA matrix when W_{PEG} was less than 10 wt %. Compared with the neat PLA, the PLA/PEG blends containing 5 and 10 wt % PEG formed more fibrils and rough fracture surfaces. This indicated that PEG was compatible with PLA and could improve the flexibility of PLA. However, when W_{PEG} was higher than 10 wt %, some white PEG granular agglomerates were observed in the PLA/PEG blends, as shown in Figure 3(d,e). This was attributed to the occurrence of phase separation in the PLA/PEG blends and further validated the results of DSC analysis. Sungsanit *et al.*[19]

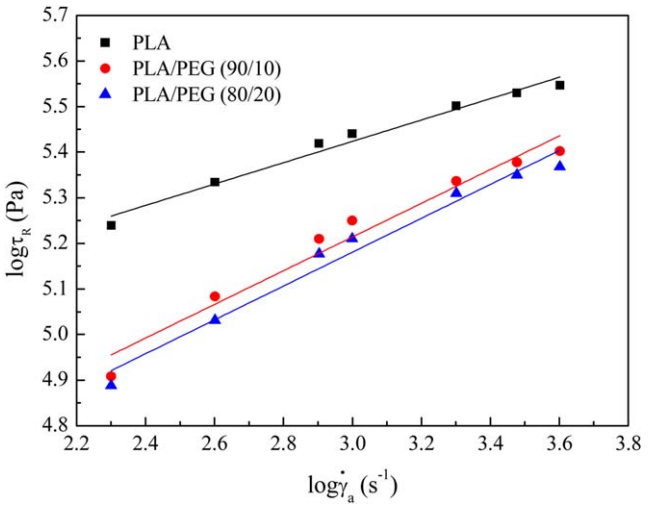

Figure 4. Flow curves of the neat PLA and PLA/PEG blend melts at 180°C. [Color figure can be viewed in the online issue, which is available at wileyonlinelibrary.com.]

reported the same results when they studied the compatibility of L-PLA/PEG 1000 blends.

Steady Shear Rheological Properties

Melt Shear Flow Curves. Melt shear flow curves present the correlation between τ_R and $\dot{\gamma}_a$, and describe the rheological behaviors of polymer melts. Figure 4 illustrates the flow curves of the neat PLA and PLA/PEG blend melts at 180°C. We observed that the log τ_R values of the neat PLA and PLA/PEG blend melts almost linearly increased with increasing log $\dot{\gamma}_a$. This indicated that the relation between τ_R and $\dot{\gamma}_a$ could be described by the following power law equation:

$$\tau_R = K\dot{\gamma}_a^n \tag{3}$$

where K is the consistency of polymer melt and n is the non-Newtonian index.

The K and n values at different shear rates are summarized in Table II, which were determined by a linear regression method. The linear correlation coefficient (R^2) of log τ_R versus log $\dot{\gamma}_a$ was greater than or equal to 0.96. The n value increased from 0.2342 to 0.3713 with increasing W_{PEG}. The result shows that the neat PLA melt and PLA/PEG blend melts belonged to pseudoplastic fluids and their pseudoplasticity decreased with increasing W_{PEG}. As is well known, K is a parameter associated with the melt viscosity. A melt with a larger K value shows that the melt viscosity is at a higher level. Because the addition of PEG played a role in diluting the PLA/PEG blend melts and could decrease the melt viscosity, the K values of the blend melts were significantly lower than that of the neat PLA, and they always declined with increasing W_{PEG}. Meanwhile, the incorporation of PEG decreased the flow resistance of the PLA/PEG blends, resulting in a decrease of the shear stress.

Effect of the Shear Rate on the Melt Shear Viscosity. Figure 5 shows the effect of $\dot{\gamma}_a$ on the apparent shear viscosity (η_a) of the neat PLA melt and PLA/PEG blend melts at 180°C. It was clear that log η_a showed a significant and nearly linear decrease with increasing log $\dot{\gamma}_a$. Namely, both the neat PLA melt and

Table II. K and n Values for the Neat PLA and PLA/PEG Blend Melts at 180°C

Samples	K (kPa·s)	n	R^2
PLA	52.6090	0.2342	0.9762
PLA/PEG (90/10)	12.7400	0.3695	0.9600
PLA/PEG (80/20)	11.6565	0.3713	0.9703

PLA/PEG blend melts exhibited obvious shear-thinning behavior. η_a is defined as the ratio of τ_R to $\dot{\gamma}_a$:

$$\eta_a = \tau_R/\dot{\gamma}_a \tag{4}$$

The following formula of η_a can be obtained by the substitution of eq. (3) into eq. (4):

$$\eta_a = K\dot{\gamma}_a^{n-1} \tag{5}$$

It is generally accepted that a decrease in the melt shear viscosity is due to disentanglement and orientation along the flow direction of polymer chains when polymeric melts are subjected to the action of increasing shear rate or τ_R. Moreover, at higher shear rates or shear stresses, the effects of disentanglement and orientation become more noticeable, and the melts exhibit apparent shear-thinning behavior.[31] Under the circumstances the flow resistance of the polymer melts decreased, and this resulted in reductions in the shear viscosities of the neat PLA and PLA/PEG blend melts.

Effect of the Temperature on the Melt Shear Viscosity. Figure 6 presents the effect of the temperature on η_a for the PLA/PEG (90/10) blend melt at different shear rates. We observed that ln η_a of the PLA/PEG blend melt increased almost linearly with increasing the reciprocal of absolute temperature (i.e., $1/T$) at a constant shear rate. This shows that the correlation between η_a and T was in accord with the following Arrhenius equation:

$$\eta_a = A_1\exp(E_1/RT) \tag{6}$$

where A_1 is the viscosity constant associated with material properties, shear rate, and stress; E_1 is the viscous flow activation

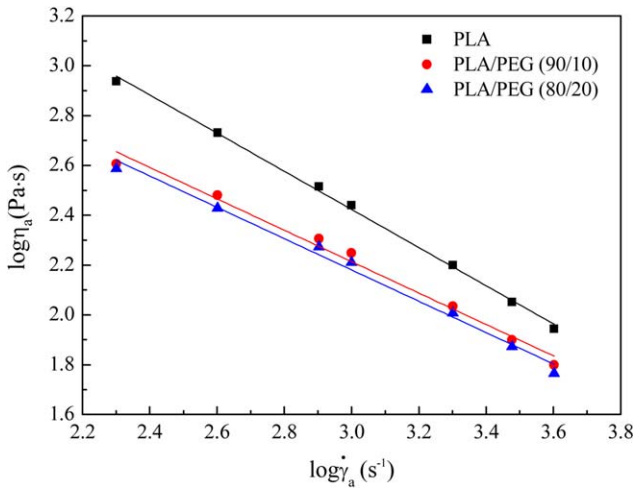

Figure 5. Effect of $\dot{\gamma}_a$ on η_a for the neat PLA and PLA/PEG blend melts at 180°C. [Color figure can be viewed in the online issue, which is available at wileyonlinelibrary.com.]

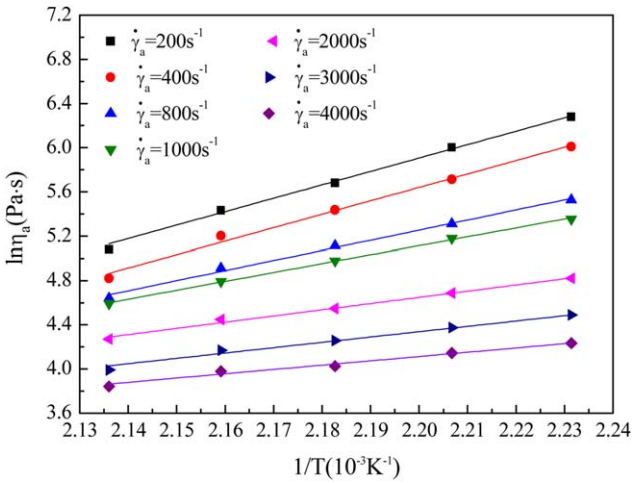

Figure 6. Effect of the temperature on η_a of the PLA/PEG (90/10) blend melt at different shear rates. [Color figure can be viewed in the online issue, which is available at wileyonlinelibrary.com.]

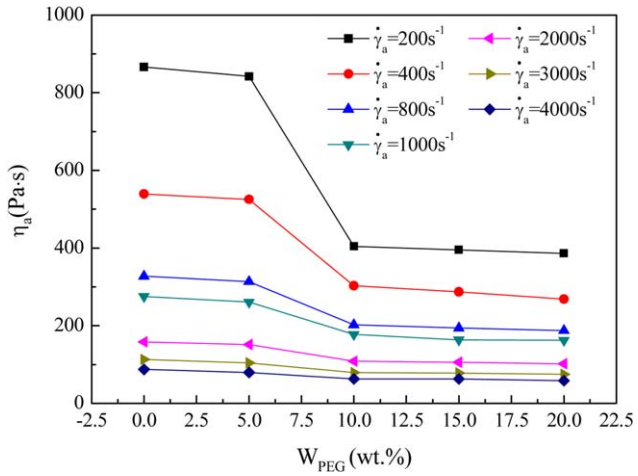

Figure 7. Effect of W_{PEG} on η_a of the PLA/PEG blend melts at 180°C and various $\dot{\gamma}_a$s. [Color figure can be viewed in the online issue, which is available at wileyonlinelibrary.com.]

energy; and R is the gas constant ($R = 8.314$ J mol^{-1} K^{-1}). Generally, the greater the E_1 value is, the higher the sensitivity of viscosity to temperature is.

On the basis of eq. (6), one can deduce the following equation:

$$\ln\eta_a = \ln A_1 + \frac{E_1}{R}\frac{1}{T} \quad (7)$$

The combination of eq. (7) with Figure 6 reveals that ln A_1 and E_1/R are the intercept and slope, respectively, of the ln η_a versus $1/T$ fitting straight line, and the A_1 and E_1 values are calculated by a linear regression method. The A_1, E_1, and R^2 values of the PLA/PEG (90/10) blend melt with $\dot{\gamma}_a$s between 200 and 4000 s^{-1} are listed in Table III.

In general, an increase in the temperature improves the capacity of molecular thermal motions; meanwhile, cavities in the melt also increase and expand, and this leads to a decrease in the flow resistance. As a result, the shear viscosity of the polymer melts decreases exponentially as the temperature rises. Table III reveals that the A_1 values increased and the E_1 values decreased with increasing $\dot{\gamma}_a$. The decreasing E_1 value indicated that η_a of the PLA/PEG (90/10) blend melt was less sensitive to temperature as $\dot{\gamma}_a$ increased. In addition, the R^2 values between ln η_a and $1/T$ exceeded 0.99.

Table III. A_1, E_1, and R^2 Values for the PLA/PEG (90/10) Blend Melt at Various Shear Rates

$\dot{\gamma}_a$ (s^{-1})	A_1 (Pa s)	E_1 (J/mol)	R^2
200	9.4020×10^{-10}	100.9420	0.9982
400	7.2302×10^{-10}	100.9292	0.9915
800	3.8340×10^{-7}	75.7434	0.9933
1000	3.5756×10^{-6}	66.7673	0.9985
2000	4.4871×10^{-4}	46.7322	0.9903
3000	1.8406×10^{-3}	40.2197	0.9957
4000	1.1686×10^{-2}	32.3769	0.9973

Effect of W_{PEG} on the Melt Shear Viscosity. Figure 7 shows the effect of W_{PEG} on the η_a of the PLA/PEG blend melts at 180°C and various $\dot{\gamma}_a$s. Under a constant shear rate, the η_a values of the PLA/PEG blend melts decreased significantly with increasing W_{PEG} when W_{PEG} was less than 10 wt %. Nevertheless, when W_{PEG} was higher than 10 wt %, η_a of PLA/PEG blend melts decreased slightly and almost linearly with increasing W_{PEG}. This was probably because the introduction of PEG played an important role in diluting PLA and hence weakened the intermolecular forces between the PLA chains. This led to a reduction in the frictional resistance (i.e., flow resistance) among the PLA molecular chains and melt layers. Meanwhile, PEG also had a good lubrication effect by decreasing the frictional resistance between the channel wall and the blend melt. For the reasons mentioned previously, it responded to the significant decrease in the shear viscosity of the blend melts. However, when the dosage of PEG reached a saturation point (i.e., solubility limit), the excess PEG in the PLA/PEG blends decreased the plasticizing and lubricating effects because of the separation of the PEG phase from the PLA matrix, as confirmed by DSC and SEM. Thus, the downtrend of shear viscosities of the PLA/PEG blend melts decreased when W_{PEG} was higher than 10 wt %.

Dynamic Rheological Properties

Influence of ω on G'. G' characterizes the energy stored in the material due to elastic deformation. Figure 8 presents the effect of ω on G' of the neat PLA and PLA/PEG blends at 180°C. We observed that the G' values of the neat PLA and PLA/PEG blends increased significantly with increasing ω. This was attributed to the increasingly imposed restrictions on the neat PLA and PLA/PEG blends. Nevertheless, the G' values of the PLA/PEG blends were lower than that of the neat PLA and decreased with increasing PEG concentration at a constant ω. As mentioned previously, PEG had a plasticization effect on PLA. When the PEG molecules were inserted into the PLA molecular chains, this weakened the interactions between the PLA molecular chains and formed additional free volumes. Consequently,

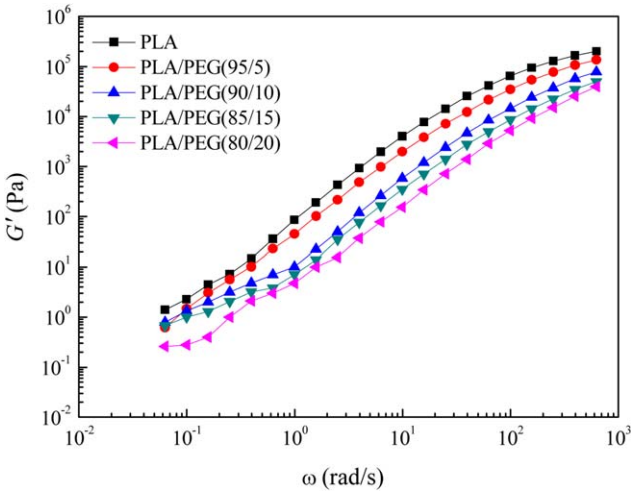

Figure 8. Influence of ω on G' of the neat PLA and PLA/PEG blends at 180°C. [Color figure can be viewed in the online issue, which is available at wileyonlinelibrary.com.]

the introduction of PEG improved the mobility of the PLA chains, and this led to a decrease in G' with increasing PEG concentration.

According to linear viscoelastic theory, the approximate relation $\log G' \propto 2 \log \omega$ in the lower ω region (terminal region) represents homogeneous polymer melts. However, the decrease in the terminal slope of $\log G'$ versus $\log \omega$ at lower frequencies shows the occurrence of phase separation and the presence of a heterogeneous structure.[23,25] The terminal slopes of the $\log G'$ versus $\log \omega$ linear regression lines of the neat PLA and PLA/PEG blends at 180°C and lower frequencies ($0.0628 \leq \omega \leq 0.628$ rad/s) are summarized in Table IV. Obviously, the terminal slopes of $\log G'$ versus $\log \omega$ of the neat PLA and PLA/PEG blends containing 5 and 10 wt % PEG were closer to 2; this indicated that the blends were homogeneous when W_{PEG} was less than 10 wt %. However, when W_{PEG} exceeded 10 wt %, the terminal slopes of $\log G'$ versus $\log \omega$ of the PLA/PEG blends were much smaller than 1; this showed that phase separation occurred in the blends. These results were consistent with DSC analysis and SEM observations.

Influence of the ω on G''. G'' characterizes the energy dissipated as heat due to viscous deformation. Figure 9 depicts the effect of ω on G'' of the neat PLA and PLA/PEG blends at 180°C. Similar to the variation of G' versus ω, the G'' values of the neat PLA and PLA/PEG blends increased remarkably with increasing ω. The reason was that the viscous response of macromolecules required more energy with increasing ω.[32] However, the G'' value of PLA/PEG blends was below that of the neat PLA and decreased with increasing W_{PEG} when ω was constant. The variation regularity of G'' with W_{PEG} could be analyzed from the following two aspects. First, the concentration of long PLA molecular chains in the PLA/PEG blend system decreased with increasing W_{PEG}; this weakened the molecular chain entanglements. Second, the plasticization and lubrication of PEG reduced the flow resistance between the PLA chain segments and improved the mobility of PLA molecular chains; this led to a decline in G''.

Table IV. Relationship between $\log G'$ and $\log \omega$ of the Neat PLA and PLA/PEG Blends at 180°C and Lower Frequencies ($0.0628 \leq \omega \leq 0.628$ rad/s)

Sample	$\log G'$ versus $\log \omega$
PLA	$\log G' \propto 1.74 \log \omega$
PLA/PEG (95/5)	$\log G' \propto 1.52 \log \omega$
PLA/PEG (90/10)	$\log G' \propto 1.36 \log \omega$
PLA/PEG (85/15)	$\log G' \propto 0.78 \log \omega$
PLA/PEG (80/20)	$\log G' \propto 0.72 \log \omega$

Relationship between W_{PEG} and the Miscibility of PEG with PLA. In the study, the Cole–Cole plot [i.e., loss viscosity (η'') versus the dynamic viscosity (η') curve] was applied to analyze the miscibility of the PLA/PEG blend melts. In general, a smooth, semicircular shape of the Cole–Cole plots shows good miscibility, namely, phase homogeneity in the melt, whereas any deviation from the shape indicates nonuniform dispersion or phase separation.[33–35] η' and η'' are, respectively, the real and imaginary parts of complex viscosity (η^*), and they are calculated according to eqs. (8) and (9):

$$\eta' = G''/\omega \quad (8)$$

$$\eta'' = G'/\omega \quad (9)$$

Figure 10 shows the Cole–Cole plots of the neat PLA and PLA/PEG blends at 180°C. We observed that the Cole–Cole curves of the neat PLA and PLA/PEG blends containing 5 and 10 wt % PEG achieved a smooth semicircular shape, respectively. However, when W_{PEG} exceeded 10 wt %, the Cole–Cole curve of the PLA/PEG blend melt was slightly smaller than a semicircle, and it became smaller with increasing W_{PEG}. This indicated that the PLA/PEG blends were miscible and homogeneous at lower W_{PEG}s ($\leq$10 wt %), whereas with the further increase in W_{PEG} (>10 wt %), phase separation occurred in the blends. These

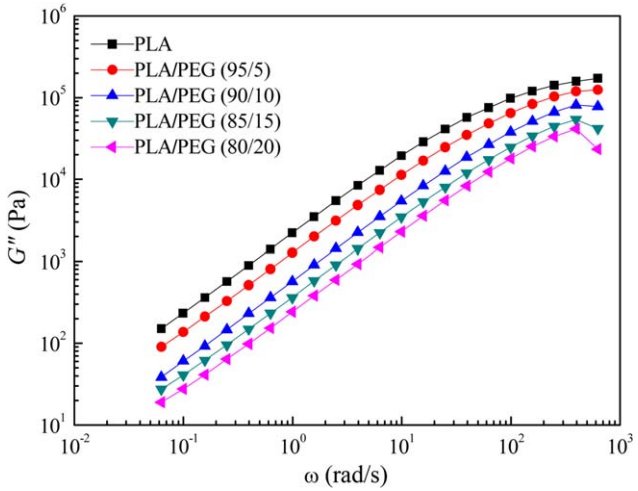

Figure 9. Influence of ω on G'' of the neat PLA and PLA/PEG blends at 180°C. [Color figure can be viewed in the online issue, which is available at wileyonlinelibrary.com.]

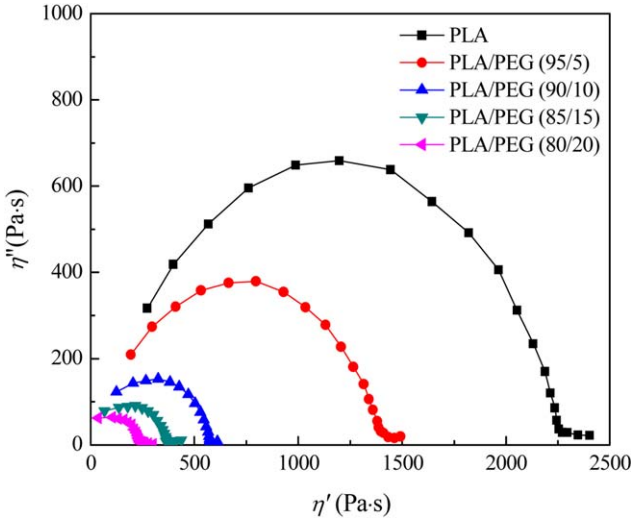

Figure 10. Cole–Cole plots of the neat PLA and PLA/PEG blends at 180°C. [Color figure can be viewed in the online issue, which is available at wileyonlinelibrary.com.]

results were in accordance with DSC analysis and SEM observations.

Influence of ω on η^*. Figure 11 shows the effect of ω on the η^* values of the neat PLA and PLA/PEG blends at 180°C. The η^* values of the neat PLA and PLA/PEG blends decreased very slightly with increasing ω when ω was less than 10 rad/s. Nevertheless, when ω increased from 10 to 628 rad/s, the η^* values of the neat PLA and PLA/PEG blends decreased significantly with increasing ω. Namely, both the neat PLA and PLA/PEG blends exhibited more significant shear-thinning behavior in the higher ω region. This showed that at higher frequencies, the η^* values of the neat PLA and PLA/PEG blends were sensitive to ω. This probably occurred because higher frequencies were conducive to the disentanglement of molecular chains, and this led to a greater decrease in the η^* values of the neat PLA and PLA/PEG blend melts.

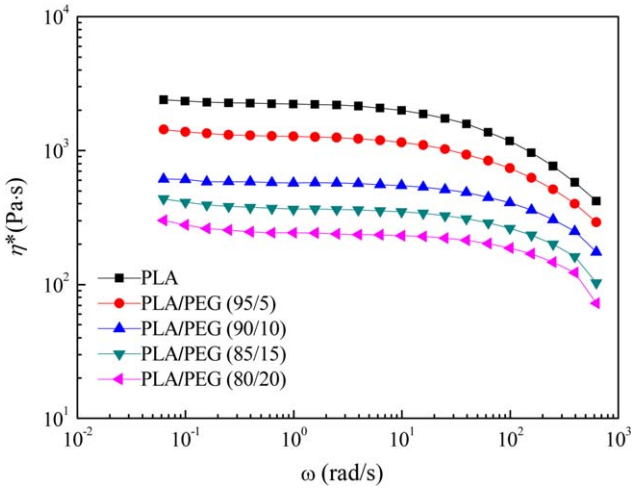

Figure 11. Influence of ω on η^* of the neat PLA and PLA/PEG blends at 180°C. [Color figure can be viewed in the online issue, which is available at wileyonlinelibrary.com.]

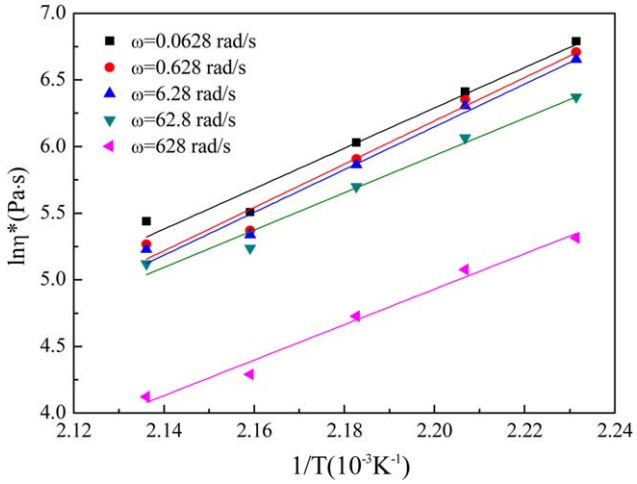

Figure 12. Influence of the temperature on η^* of the PLA/PEG (90/10) blend melt at various frequencies. [Color figure can be viewed in the online issue, which is available at wileyonlinelibrary.com.]

Influence of Temperature on η^*. Figure 12 illustrates the temperature dependence of η^* of the PLA/PEG (90/10) blend melt at various frequencies. Similar to the variation of ln η_a versus $1/T$ (see Figure 6), ln η^* of the PLA/PEG blend melt increased nearly linearly with increasing $1/T$ at a constant ω. This indicated that the relationship between η^* and T conformed to the Arrhenius equation:

$$\eta^* = A_2 \exp(E_2/RT) \tag{10}$$

where A_2 is the viscosity constant, E_2 is the viscous flow activation energy, and R is the gas constant. In general, a greater E_2 value indicates that η^* of the melt is more sensitive to temperature. Taking the natural logarithm on both sides of eq. (10), we can obtain the following equation:

$$\ln\eta^* = \ln A_2 + \frac{E_2}{R}\frac{1}{T} \tag{11}$$

The A_2 and E_2 values of PLA/PEG (90/10) blend melt was determined by a linear regression method, and their values in the ω range from 0.0628 to 628 rad/s are summarized in Table V. We observed that the A_2 value increased, whereas the E_2 value decreased with increasing ω. This was because with increasing ω, the effects of disentanglement and orientation of the polymer chains became more remarkable and the PLA/PEG blend melt exhibited shear-thinning behavior. Under the circumstances, the flow resistance of polymer melt decreased, and

Table V. A_2, E_2, and R^2 Values of the PLA/PEG (90/10) Blend Melts at Various Frequencies

ω (rad/s)	A_2 (Pa s)	E_2 (J/mol)	R^2
0.0628	1.7899×10^{-12}	126.0809	0.9597
0.628	1.4465×10^{-13}	135.2276	0.9654
6.28	2.1464×10^{-13}	133.5655	0.9673
62.8	1.6402×10^{-11}	116.3565	0.9726
628	2.6382×10^{-11}	110.7624	0.9791

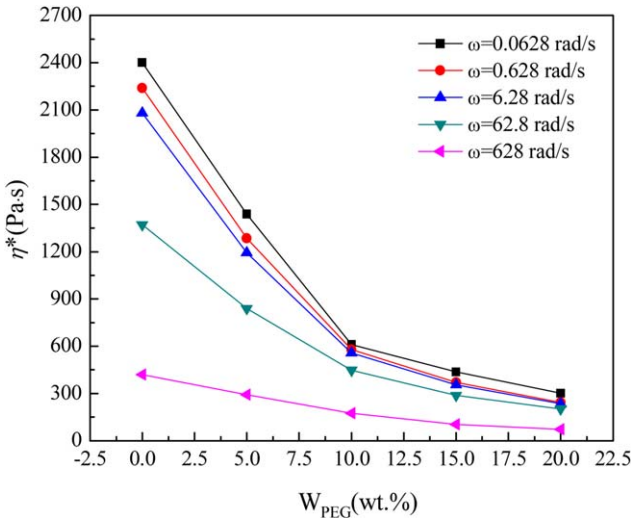

Figure 13. Influence of W_{PEG} on η^* of the PLA/PEG blends at 180°C and various frequencies. [Color figure can be viewed in the online issue, which is available at wileyonlinelibrary.com.]

this led to a decrease in E_2 of the PLA/PEG blend melt. The decreased E_2 value implied that η^* of the PLA/PEG blend melt was less sensitive to temperature as ω increased. Additionally, the R^2 between ln η^* and $1/T$ were greater than 0.95.

Influence of W_{PEG} on η^*. Figure 13 displays the influence of W_{PEG} on η^* of the PLA/PEG blends at 180°C and various frequencies. Similar to the variation trends of η_a versus W_{PEG} (see Figure 7), η^* of the PLA/PEG blends was lower than that of the neat PLA and decreased dramatically with increasing W_{PEG} when W_{PEG} was less than 10 wt %. Nevertheless, when W_{PEG} was higher than 10 wt %, η^* of the PLA/PEG blends decreased slightly with increasing W_{PEG} at a constant ω. This was probably because PEG had dilution and lubrication effects on PLA. When W_{PEG} was less than 10 wt %, the complete miscibility of PEG and PLA [see Figure 3(b,c)] was likely to result in the interaction of well-dispersed PEG molecules with the PLA chain; this weakened the intermolecular forces between the PLA chains and thereby decreased chain entanglements. Meanwhile, it increased the free volume and segmental mobility of the PLA chains and led to a significant reduction in η^* of the PLA/PEG blend melts with increasing PEG concentration. However, when the PEG concentration reached a saturation point, excess PEG (>10 wt %) played relatively weaker roles in plasticization and lubrication because of the incomplete miscibility of PEG and PLA [see Figure 3(d,e)]. Consequently, the downward trends of η^* of the PLA/PEG blend melts lessened when W_{PEG} exceeded 10 wt %.

CONCLUSIONS

In this study, DSC, SEM, and rheological tests were used to explore the phase separation of PLA/PEG blends. The SEM observations, DSC, and Cole–Cole analysis demonstrated that the miscibility of PEG with PLA depended on the PEG concentration. At lower PEG concentrations (≤10 wt %), the PEG particles were homogeneously and finely dispersed in the PLA matrix. Nevertheless, when the PEG concentration exceeded 10 wt %, PEG phase separated from the PLA matrix. Furthermore, the rheological results revealed that the melt shear flow of the neat PLA and PLA/PEG blends obeyed the power law, whereas the dependence of η_a or η^* on T could be described by the Arrhenius equation. Both the neat PLA melt and PLA/PEG blend melts exhibited shear-thinning behavior. Compared to neat PLA, the incorporation of PEG weakened the intermolecular forces and improved the mobility of the PLA chains. As a result, it reduced the η_a, η^*, G', and G'' values of the PLA/PEG blends. Moreover, the G' and G'' values of the neat PLA and PLA/PEG blends significantly increased, whereas η^* decreased with increasing ω. The plasticization and lubrication efficiencies of PEG were relevant to W_{PEG}. When W_{PEG} was less than 10 wt %, both η_a and η^* of the PLA/PEG blends decreased remarkably with increasing W_{PEG} and then decreased slightly as W_{PEG} increased further because of the occurrence of phase separation. This indicated that the introduction of the right amount of PEG was very effective in enhancing the compatibility and flow properties of PLA.

ACKNOWLEDGMENTS

The authors acknowledge the financial support from the National Science Fund (50903032 and U1333126), a Fund Research Grant for Science and Technology in Guangzhou, China (2014J4100038), the Fundamental Research Funds for the Central Universities (2015ZZ020), and the Opening Project of the Key Laboratory of Polymer Processing Engineering (Ministry of Education, China).

REFERENCES

1. Rasal, R. M.; Janorkar, A. V.; Hirt, D. E. *Prog. Polym. Sci.* **2010**, *35*, 338.
2. Saeidlou, S.; Huneault, M. A.; Li, H. B.; Park, C. B. *Prog. Polym. Sci.* **2012**, *37*, 1657.
3. Zhao, Q. N.; Ding, Y.; Yang, B.; Ning, N. Y.; Fu, Q. *Polym. Test.* **2013**, *32*, 299.
4. Nampoothiri, K. M.; Nair, N. R.; John, R. P. *Bioresour. Technol.* **2010**, *101*, 8493.
5. Okamoto, M.; John, B. *Prog. Polym. Sci.* **2013**, *38*, 1487.
6. Arrieta, M. P.; López, J.; Ferrándiz, S.; Peltzer, M. A. *Polym. Test.* **2013**, *32*, 760.
7. Chien, Y. C.; Liang, C. J.; Yang, S. H. *Atmos. Environ.* **2011**, *45*, 123.
8. Drumright, R. E.; Gruber, P. R.; Henton, D. E. *Adv. Mater.* **2000**, *12*, 1841.
9. Grijpma, D. W.; Nijenhuis, A. J.; Van Wijk, P. G. T.; Pennings, A. *J. Polym. Bull.* **1992**, *29*, 571.
10. Liu, G. C.; He, Y. S.; Zeng, J. B.; Li, Q. T.; Wang, Y. Z. *Biomacromolecules* **2014**, *15*, 4260.
11. Liang, J. Z.; Duan, D. R.; Tang, C. Y.; Tsui, C. P.; Chen, D. Z. *Polym. Test.* **2013**, *32*, 617.
12. He, Y. S.; Zeng, J. B.; Liu, G. C.; Li, Q. T.; Wang, Y. Z. *RSC Adv.* **2014**, *4*, 12857.
13. Liu, G. C.; He, Y. S.; Zeng, J. B.; Xu, Y.; Wang, Y. Z. *Polym. Chem.* **2014**, *5*, 2530.

14. Shibata, M.; Inoue, Y.; Miyoshi, M. *Polymer* **2006**, *47*, 3557.
15. Jiang, L.; Wolcott, M. P.; Zhang, J. W. *Biomacromolecules* **2006**, *7*, 199.
16. Kang, H. L.; Qiao, B.; Wang, R. G.; Wang, Z.; Zhang, L. Q.; Ma, J.; Coates, P. *Polymer* **2013**, *54*, 2450.
17. Zhang, W.; Chen, L.; Zhang, Y. *Polymer* **2009**, *50*, 1311.
18. Martin, O.; Averous, L. *Polymer* **2001**, *42*, 6209.
19. Sungsanit, K.; Kao, N.; Bhattacharya, S. N. *Polym. Eng. Sci.* **2012**, *52*, 108.
20. Kulinski, Z.; Piorkowska, E.; Gadzinowska, K.; Stasiak, M. *Biomacromolecules* **2006**, *7*, 2128.
21. Labrecque, L. V.; Kumar, R. A.; Davé, V.; Gross, R. A.; McCarthy, S. P. *J. Appl. Polym. Sci.* **1997**, *66*, 1507.
22. Jacobsen, S.; Fritz, H. G. *Polym. Eng. Sci.* **1999**, *39*, 1303.
23. Thompson, M. S.; Vadala, T. P.; Vadala, M. L.; Lin, Y.; Riffle, J. S. *Polymer* **2008**, *49*, 345.
24. Sheth, M.; Kumar, R. A.; Davé, V.; Gross, R. A.; Mccarthy, S. P. *J. Appl. Polym. Sci.* **1997**, *66*, 1495.
25. Du, M.; Gong, J. H.; Zheng, Q. *Polymer* **2004**, *45*, 6725.
26. Utracki, L. A. Polymer Alloys and Blends; Hanser: New York, **1989**; p 131.
27. Zheng, Q.; Du, M.; Yang, B. B.; Wu, G. *Polymer* **2001**, *42*, 5743.
28. Li, Y. L.; Li, X. X.; Xiang, F. M.; Huang, T.; Wang, Y.; Wu, J.; Zhou, Z. W. *Polym. Adv. Technol.* **2011**, *22*, 1959.
29. Cuénoud, M.; Bourban, P. E.; Plummer, C. J. G.; Manson, J. A. E. *J. Appl. Polym. Sci.* **2011**, *121*, 2078.
30. Li, F. J.; Zhang, S. D.; Liang, J. Z.; Wang, J. Z. *Polym. Adv. Technol.* **2015**, *26*, 465.
31. Liang, J. Z.; Tang, C. Y.; Zhou, L.; Tsui, C. P.; Li, F. *J. Polym. Eng. Sci.* **2012**, *52*, 1839.
32. Prut, E.; Kuznetsova, O.; Karger-Kocsis, J.; Solomatin, D. J. *Reinf. Plast. Compos.* **2012**, *31*, 1758.
33. Cho, K.; Lee, B. H.; Hwang, K. M.; Lee, H.; Choe, S. *Polym. Eng. Sci.* **1998**, *38*, 1969.
34. Ahmed, J.; Varshney, S. K.; Auras, R.; Hwang, S. W. *J. Food Sci.* **2010**, *75*, N97.
35. Joshi, M.; Butola, B. S.; Simon, G.; Kukaleva, N. *Macromolecules* **2006**, *39*, 1839.